

# On Inferential Iterative Learning Control: with Example to a Printing System

Joost Bolder, Tom Oomen, and Maarten Steinbuch

**Abstract**—Since performance variables cannot be measured directly, Iterative Learning Control (ILC) is usually applied to measured variables. In this paper, it is shown that this can deteriorate performance. New batch-wise sensors that measure the performance variables directly are well-suited for use in ILC and can potentially improve performance. In this paper, recent developments in inferential control are utilized to arrive at control structures suited for inferential ILC. The proposed frameworks extend earlier results and encompass various controller structures. The results are supported with a simulation example.

## I. INTRODUCTION

In many physical systems, the variables that define the performance cannot be measured directly in real-time. This may for instance stem from constraints on sensor cost, from physical limitations in sensor placement, or from computational constraints. In inferential feedback control, the performance has to be inferred from the measured variables with models, and is therefore inherently determined by model accuracy, see [1] for inferential control in the process industry, and [2], [3] for identification and robust inferential control of mechatronic systems.

An example of a system where the performance cannot be measured in real-time is the Medium Positioning Drive (MPD) in a wide-format printer [4]. In this system, the measured variable is the motor position, and performance is defined as the medium position at the printheads. The dynamics of the MPD cause differences between the measured and performance variables. Recently, a sensor has been introduced that can measure the performance directly, but offline in a batch-to-batch fashion. This measurement is therefore not suited for traditional real-time feedback control. However, it is well-suited for batch-wise control strategies such as Iterative Learning Control (ILC) [5]–[8].

Although conceptually well-suited, extending the feedback controlled system with a batch-wise ILC controller is not straightforward. The objective of feedback controller is to achieve tracking in the measured variable, where the objective of the ILC is to achieve tracking in the performance variable, possibly creating a conflict. The objective is to analyze this control setting.

Related work, see [9], considers using accelerometers with an observer to improve performance of an lab-scale robot arm. This idea is further extended in [10] where a framework for observer-based ILC is presented, where the

observer is used to reconstruct the performance variables. Although the related results in [9], [10] address the difference between measured and performance variables, estimating the performance variables using an observer is a specific choice of dealing with the inferential control problem. Pre-existing feedback structures for inferential control include the use of an observer as a special case.

This paper thoroughly analyzes inferential ILC, and it is shown that more general solutions exist that effectively deal with the inferential control setting. This enables the systematic design of both feedback and feedforward controllers with inferential control.

The contributions of the present paper are threefold. Firstly, the traditional feedback with feedforward control structure in the inferential control setting is analyzed. Secondly, the so-called two-Degree-Of-Freedom (2-DOF) inferential feedback structure is extended with ILC. Thirdly, the common one-Degree-Of-Freedom (1-DOF) feedback controller structure is extended with ILC, where the inferential control situation is specifically addressed. The norm-optimal ILC framework is used, and a mathematical performance analysis is presented, with the system subject to disturbances. The analysis is supported with a simulation study using an identified model of the MPD.

This paper is organized as follows. The aspects of common 1-DOF feedback and feedforward controllers in the inferential control setting are investigated in the problem definition in Section II. A 2-DOF feedback with ILC solution is proposed in Section III. A solution in the 1-DOF structure is proposed in Section IV. The results are supported with a simulation example in Section V. Finally, the conclusions are presented in Section VI.

*Notation:* all signals and systems are discrete time and often implicitly assumed of length  $n$ . The  $i^{\text{th}}$  element of a vector  $\theta$  is expressed as  $\theta(i)$ . A matrix  $A \in \mathbb{R}^{n \times n}$  is defined positive definite iff  $x^T A x > 0, \forall x \in \mathbb{R}^n, x \neq 0$  and is denoted as  $A \succ 0$ . For a vector  $x \in \mathbb{R}^n$ , the weighted 2-norm is  $\|x\|_W = x^T W x$ , with  $W \succ 0 \in \mathbb{R}^{n \times n}$  the weighting matrix. Given, is a system  $H$ , and finite-time input and output vectors  $u, y \in \mathbb{R}^{n \times 1}$ . Let  $h(t), t \in \mathbb{Z}$  be the impulse response of  $H$ . The finite-time response of  $H$  to  $u$  is given by the truncated convolution  $y(t) = \sum_{l=1-n}^t h(l)u(t-l)$ , with  $0 \leq t < n$ , and zero initial conditions. This finite-time convolution is recast to  $y = H u$ , with  $H$  the convolution matrix corresponding to system  $H$ , and  $y$  the finite time response. Note that  $H$  is not restricted to be a causal system, otherwise  $h(t < 0) = 0$ .

The authors are with the Eindhoven University of Technology, Dept. of Mechanical Engineering, Control Systems Technology group, P.O. Box 513, 5600 MB Eindhoven, The Netherlands, j. j. bolder@tue.nl

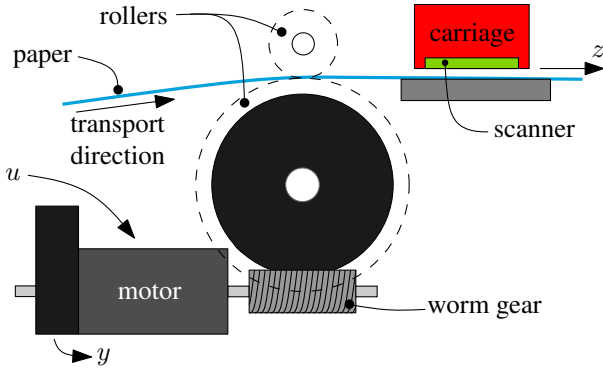


Fig. 1. Medium positioning drive: the motor is driven with voltage  $u$ , the rotor position  $y$  is measured using an optical encoder, the paper is transported by the rollers and the paper position  $z$  is measured using the scanner inside the carriage.

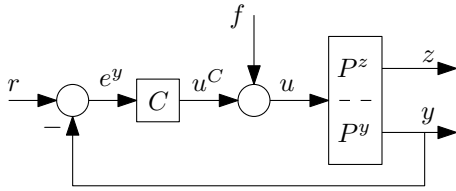


Fig. 2. Conventional feedback control structure with feedforward  $f$ .

## II. COMBINING INFERENTIAL ILC AND CLASSICAL FEEDBACK: POTENTIAL HAZARDS

The relevance of the problem addressed in this paper is clarified using the example motion system in Fig. 1. The system is a Medium Positioning Drive (MPD) in a wide-format inkjet printer [4]. The task of the system is to accurately position the paper. The performance variable  $z$  is defined as the paper position at the carriage (that holds the print-heads). The measured variable is the motor position  $y$ , and the motor is driven through input  $u$ .

Often, such systems are controlled using a one-Degree-Of-Freedom (1-DOF) feedback control loop with feedforward, as is shown in Fig. 2. The feedback controller  $C$  determines  $u$  using the tracking error  $e^y = r - y$ . Typically,  $C$  is designed such that  $e^y$  is small in some sense. The system  $P$  has two outputs,  $z = P^z u$  and  $y = P^y u$ . The systems  $P^z$  and  $P^y$  may have common dynamics, i.e., they do not need to be decoupled. For clarity of explanation, the feedforward is assumed zero for now.

The performance is determined by  $e^z = r - z$ , assuming that  $\dim z(t) = \dim y(t)$ , as is the case with the MPD. Suppose that the feedback controller achieves  $e^y = 0$ . The latter implies that  $y = r$ , and from Fig. 2 results  $u = (P^y)^{-1}r$ . Consequently,  $z = P^z(P^y)^{-1}r$ . Substituting the latter in the performance yields  $e^z = (1 - P^z(P^y)^{-1})r$ . This example illustrates that if  $P^z \neq P^y$ , then achieving  $e^y = 0$  introduces performance degradation since it directly implies  $e^z \neq 0$ , see [11, Section 3.3.2] for more details.

The MPD has recently been equipped with scanner in the carriage, see Fig. 1. The scanner records an image of the paper during operation. An image processing algorithm

determines the paper displacement  $z$  from the scans; offline in a batch-to-batch fashion. Iterative Learning Control (ILC) is a control strategy that updates the feedforward offline in a batch-to-batch fashion and is hence well-suited to be used in combination with the offline performance measurements.

Iterative Learning Control is able to achieve very good tracking performance. Suppose that the feedforward  $f$  is optimized with ILC using the scans, i.e.,  $z$  is measured, reaching  $e^z = r - z = 0$ . The latter implies  $u^* = (P^z)^{-1}r$ , the corresponding optimal feedforward  $f^*$ , feedback signal  $u^{C^*}$ , and  $e^y$  are formulated in Proposition 1.

**Proposition 1.** *Given  $r$ ,  $C$ ,  $P^z$ , and  $P^y$ , the feedforward that attains  $e^z = 0$  is given by  $f^* = (P^z)^{-1}r - C(1 - P^y(P^z)^{-1})r$ . The corresponding feedback control effort  $u^{C^*} = C(1 - P^y(P^z)^{-1})r$ . The performance is optimal since  $e^z = 0$ , the latter implies  $z = r$  and therefore  $e^y = (1 - P^y(P^z)^{-1})r$ .*

*Proof.* From Fig. 2 follows  $e^z = r - z = (1 - P^z C S)r - P^z S f$  with  $S := (1 + C P^y)^{-1}$ , solving  $e^z = 0$  for  $f$  yields  $f^*$ . The rest follows from substitution of  $f^*$  in the loop equations that can be derived from Fig. 2.  $\square$

Proposition 1 illustrates that optimal performance can be attained reaching  $e^z = 0$  by using a conventional feedback control loop with feedforward in an inferential control setting. However, the feedback controller is designed to reduce  $e^y$ , and the feedforward is designed such that  $e^z = 0$ . The latter indicates a potential conflict, this conflict is illustrated with the following example.

Suppose that  $C$  is a high-performance controller and hence includes pure integrators, i.e.,  $|C(z=1)| = \infty$ , let  $r(t) = c_1$  and  $P^y = c_2 P^z$ , with  $c_1$  and  $c_2$  constants. Then from Proposition 1 follows  $u^{C^*} = C(1 - c_2)c_1$ . Since  $(1 - c_2)c_1$  is constant and  $C$  includes integrators, the feedback control effort  $u^{C^*}$  is a signal that grows unbounded when  $t \rightarrow \infty$ . The feedforward can be recast to  $f^* = (P^z)^{-1}c_1 - u^{C^*}$ , consequently, the feedforward grows unbounded as well, with opposite sign. This behavior is however unobserved at the input to the process, since  $u^* = (P^z)^{-1}r$ . Essentially, the feedforward is canceling the feedback control effort. The ILC is able to compensate the feedback controller since it includes a model of the closed-loop, see [12].

A potential problem occurs if the feedback controller is redesigned, and the feedforward is kept the same. Indeed, since  $u = f^* + u^C$ , with  $f^*$  an unbounded signal, and the new  $u^C$  a different signal as before, the feedforward is not exactly canceling the feedback control effort. Consequently, the input to the process could grow unbounded, which is undesired for obvious safety reasons.

These examples illustrate several key issues that occur when using a common control structure in an inferential control setting:

- the feedforward may be conflicting with the feedback controller
- the optimal feedforward is a function of the feedback controller

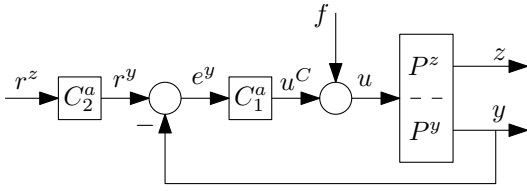


Fig. 3. 2-DOF feedback control structure for inferential control.

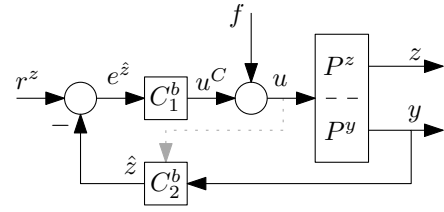


Fig. 4. Different 2-DOF feedback control structure for inferential control.

- the optimal signals  $f$  and  $u^C$  may posses undesired characteristics
- safety issues could occur if the feedback controller changed and the feedforward signal is kept the same (i.e.,  $f$  is not reset after changing  $C$ )

The conflicting objectives are a result of using a parallel ILC and feedback controller structure [5], which is common in motion control. As will be shown, using a serial configuration eliminates the conflicting objectives, at the expense of a converged ILC command signal that depends on the  $C$ . In the present paper, these aspects will be addressed accordingly:

- 1) a two-degree-of-freedom feedback with ILC solution is presented in Section III, involving redesign of the feedback controller,
- 2) an alternative one-degree-of-freedom feedback with ILC solution with is presented in Section IV, assuming the feedback controller must remain unchanged,

The presented solutions and analysis are supported with a numerical example in Section V, where a model of the system in Fig. 1 is used.

### III. 2-DOF CONTROLLER STRUCTURES FOR INFERENCEIAL ILC

In Section III-A, the single-degree-of-freedom (1-DOF) feedback control structure in Fig. 2 is extended to a two-degrees-of-freedom (2-DOF) control structure. Then, ILC is introduced in Section III-B. Finally, an analysis of the performance is presented in Section III-C.

#### A. 2-DOF inferential feedback stuctures

As argued in Section II, single-degree-of-freedom (1-DOF) feedback control structures such as in Fig. 2 are not suited for high-performance servo control due to the fact that feedback control using the measured variable  $y$  does not imply adequate performance, determined by  $z$ . Moreover, the 1-DOF control structure can only deal with the situation where  $\dim z(t) = \dim y(t)$ . To this end, two-Degree-Of-Freedom (2-DOF) structures are introduced and presented in Fig. 3 and Fig. 4.

The structure in Fig. 3 is known as indirect control [13, Section 10.4.2]. The controller  $C_2^a$  can be interpreted as a transformation of the reference  $r^z$  to a reference  $r^y$ . Here  $C_1^a$  can be seen as the conventional feedback controller. The controller  $C_2^a$  is designed using a model of  $P^z, P^y$ . Ideally,  $C_2^a = P^y(P^z)^{-1}$ . Indeed, in the absence of disturbances, the latter implies  $r^y - y = 0 \Leftrightarrow r^z - z = 0$ . Any modeling error in  $P^y(P^z)^{-1}$  directly results in performance degradation. If the reference  $r^z$  is known a priori, the stable inversion

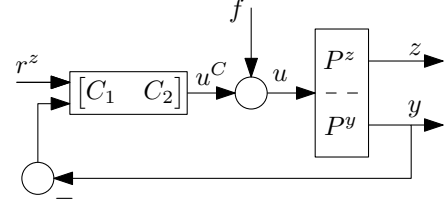


Fig. 5. Unifying 2-DOF feedback control structure for inferential control.

approach in [14] can be adopted to calculate  $P^y(P^z)^{-1}r^z$  in case of non-minimum phase  $P^z$  and/or unstable  $P^y$ .

The structure in Fig. 4 is the situation where the  $z$  variable is inferred in real-time from the measurement  $y$  by controller  $C_2^b$ , and known as inferential control [1]. Here,  $C_2^b$  could for instance be an observer (possibly needing access to  $u$ , indicated with the dotted arrow in Fig. 4). The controller  $C_1^b$  can be seen as the conventional feedback controller, but now using an inferred performance variable  $\hat{z}$  from measurement  $y$ . The relation between modeling errors and performance degradation is less transparent than with the indirect control structure in Fig. 3, since it depends on the estimation error of the observer, see, e.g., [15]. A static transformation  $C_2^b = P^z(P^y)^{-1}$ , similar to the indirect control situation can also be used, with the restriction that  $C_2^b$  must be stable since  $\hat{z}$  must be calculated online.

These controller structures are captured in a unifying inferential control scheme, presented in Fig. 5. The conventional 1-DOF feedback structure in Fig. 2, and 2-DOF structures in Fig. 3 and Fig. 4 are special cases by setting

$$\begin{aligned} [C_1 \ C_2] &= [C \ C], \\ [C_1 \ C_2] &= [C_2^a C_1^a \ C_1^a], \\ [C_1 \ C_2] &= [C_1^b \ C_2^b C_1^b], \end{aligned}$$

respectively. The suggested choices for  $C_2^a = P^y(P^z)^{-1}$  and  $C_2^b = P^z(P^y)^{-1}$  are equivalent in the structure of Fig. 5 with  $C_1 = P^y(P^z)^{-1}C_2$ .

As is illustrated in this section, relevant design choices for the 2-DOF controller include an observer or a model-based transformation of the reference, see [11] for more details. The achieved performance inherently depends on model accuracy. Identification techniques for robust inferential control have been developed in [2] and [3].

Extension of the 2-DOF controller in Fig. 5 towards ILC is motivated by the example system in the problem formulation, see Section II, and is elaborated on in the next section.

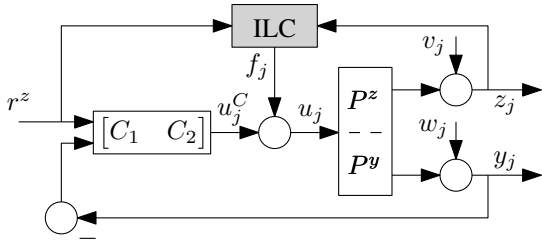


Fig. 6. Unifying 2-DOF feedback control structure with ILC for inferential control.

### B. 2-DOF feedback with ILC

As is argued in the previous section, the performance of 2-DOF feedback structures is inherently coupled to the model quality of  $P^z, P^y$ , since real-time measurements of the performance variable are unavailable. The example system presented in the problem formulation, see Section II, incorporates offline batch-to-batch measurements of  $z$ , and hence, this measurement is not suited for use in a feedback loop. Although unsuited for feedback, the measurement is very suited for use with ILC.

The extended control structure is presented in Fig. 6. Each batch is a separate experiment, also called trial. The trial index is denoted  $j$ . The signal  $f_j$  is updated by the ILC by using the offline measurement  $z_j$ . Unknown, possibly trial-varying, disturbances  $v_j$  and  $w_j$  have been included to analyze the effects of disturbances on the performance. The ILC algorithm is given by:

$$f_{j+1} = L e_j^z + Q f_j, \quad (1)$$

with  $L$  and  $Q$  the learning matrices and the performance variable  $e_j^z = r^z - z_j$ . A common algorithm to analytically compute the  $L$  and  $Q$  matrices from an optimization criterion is norm-optimal ILC [16]–[19]. The cost function adopted in this paper is as follows:

$$\mathcal{J}(f_{j+1}) := \|e_{j+1}^z\|, \quad (2)$$

yielding an inverse-model ILC.

### C. Performance analysis

The following is a performance analysis of inverse-model ILC, that minimizes  $\mathcal{J}$ . Given are the following assumptions:

- 1) the convolution matrices of  $P^z, S$  and  $C$  are invertible, such that inverse-model learning matrices  $L$  and  $Q$  exist,
- 2) the models  $P^z, P^y$  represent the exact system,
- 3) the 2-DOF feedback controller is designed as is suggested in Section III-A, with  $C_1 = P^y(P^z)^{-1}C_2$ .

The first assumption is non-restrictive and allows a practically relevant performance analysis. If  $P^z$  or  $S$  does not have full rank, then the cost function can be extended to include an arbitrary small penalty on  $f_{j+1}$  or  $f_{j+1} - f_j$ , this ensures the existence of the learning matrices  $L, Q$ , at the expense of a small degradation in tracking performance or convergence speed, respectively. The second assumption is less realistic in practice and has consequences for both the ILC and 2-DOF feedback controller. The convergence criterion of

the ILC requires  $\|(I - LP^zS)\| < 1$ , if this criterion is satisfied, modeling errors mostly affect convergence speed [5]. Considering the 2-DOF feedback controller: modeling errors introduce performance degradation and therefore requires identification techniques for robust inferential control [2] and [3]. In practice, the converged signals with a inverse-model norm-optimal ILC can be close to the results presented here, given that accurate models are identified.

The inverse-model ILC learning matrices that minimize (2) are  $L = [P^zS]^{-1}$  and  $Q = I$ , with  $S := (1 + C_2P^y)^{-1}$ . In the following theorem, the relevant signals of trial  $j + 1$  as function of the measurement data of trial  $j$  are given.

**Theorem 2.** *Given measurements  $e^z$ , disturbances  $w_j, w_{j+1}, v_j, v_{j+1}$ , the reference  $r^z$ , let the assumptions 1-3 hold, and given  $L, Q$ , then the signals  $f_{j+1}, e_{j+1}^z, u_{j+1}$  and  $y_{j+1}$  are given by:*

$$\begin{aligned} f_{j+1} &= (P^z)^{-1}r^z + C_2w_j - Lv_j, \\ e_{j+1}^z &= P^zSC_2(w_{j+1} - w_j) - (v_{j+1} - v_j), \\ u_{j+1}^C &= C_1v_j - C_2(Sw_{j+1} + Tw_j), \\ y_{j+1} &= P^y(P^z)^{-1}r^z - P^y(P^z)^{-1}v_j + Tw_j + Sw_{j+1}. \end{aligned}$$

*Proof.* From Fig. 6 follows  $u_j = Sf_j + SC_1r^z - SC_2w_j$ ,  $e_j^z = (I - P^zSC_1)r^z - P^zSf_j + P^zSC_2w_j - v_j$  and  $u_{j+1}^C = u_{j+1} - f_{j+1}$ . Substitution of  $e_j^z$  in (1) yields  $f_{j+1}$ . The result follows by substitution of  $f_{j+1}$  in  $u_{j+1}^C$  and  $y_{j+1}$ .  $\square$

Theorem 2 shows that only  $f_{j+1}$  depends on  $r^z$ , and  $u_{j+1}^C$  does not. If the disturbances are trial-invariant, i.e.,  $w_{j+1} = w_j = w$  and  $v_{j+1} = v_j = v$ , then the tracking error  $e_{j+1}^z = 0$ , yielding perfect tracking performance. The output  $y_{j+1} = P^y(P^z)^{-1}r^z + w - P^y(P^z)^{-1}v + w$  and feedback control effort  $u_{j+1}^C = C_1v$ .

**Corollary 3.** *If the disturbances are zero, the feedforward reduces to  $f_{j+1} = (P^z)^{-1}r^z$ , and is only depended on the system. The latter is useful since adjustment of the feedback controller does not affect the optimal feedforward.*

**Remark 1.** *The analysis shows that in the case of trial-invariant disturbances, the feedback control effort  $u_{j+1}^C = C_1v - C_2w$ . The corresponding feedforward  $f_{j+1} = (P^z)^{-1}r^z + C_2w - Lv$ . The latter shows that  $u_{j+1}^C$  has a term  $-C_2w$  and  $f_{j+1}$  a term  $C_2w$ . Consequently, a conflict as is illustrated in Proposition 1 may still occur. In that case, it may be relevant to design  $C_2$  such that  $C_2w$  is small in some sense. The framework proposed in the next section does not suffer from such a conflict, at the expense of a ILC command signal that depends on  $C$ .*

## IV. A 1-DOF FEEDBACK CONTROL STRUCTURE FOR INFERENCE ILC

In certain controller environments, it may be impossible to change the feedback controller, as is required in Section III. In this section, a common 1-DOF feedback control structure is considered, and the ILC is designed specifically to deal with the inferential control situation.

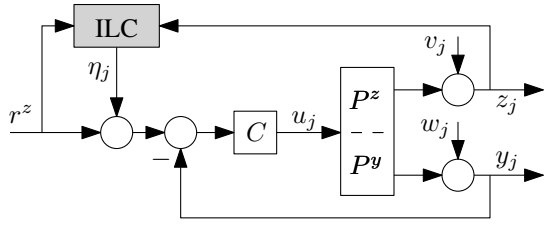


Fig. 7. Common 1-DOF feedback control structure with ILC for inferential control.

### A. 1-DOF inferential ILC framework

The 1-DOF inferential ILC structure is presented in Fig. 7. The ILC command signal is denoted as  $\eta_j$  and is placed in a serial configuration with the feedback loop. The main idea is that the ILC determines  $\eta_j$ , that is added to  $r^z$ , such that  $e^z = r^z - z = 0$  is achieved. The learning update is given by:

$$\eta_{j+1} = L e_j^z + \eta_j \quad (3)$$

### B. Performance analysis

An identical performance analysis as in Section III-C is performed. Let the assumptions Section III-C in hold. The learning matrices that minimize (2) are  $L = [P^z S C]^{-1}$  and  $Q = I$ , with  $S := (1 + C P^y)^{-1}$ . The following theorem formulates the relevant signals of trial  $j + 1$  as function of the measurement data of trial  $j$ .

**Theorem 4.** Given measurements  $e^z$ , disturbances  $w_j, w_{j+1}, v_j, v_{j+1}$  and the reference  $r^z$ , let the assumptions 1-3 in Section III-C hold, and given  $L, Q$ , then the signals  $\eta_{j+1}, e_{j+1}^z, u_{j+1}$  and  $y_{j+1}$  are given by:

$$\begin{aligned} \eta_{j+1} &= (L - I)r^z + w_j - L v_j, \\ e_{j+1}^z &= -(v_{j+1} - v_j) + P^z S C (w_{j+1} - w_j), \\ u_{j+1} &= (P^z)^{-1} r^z - S C (w_{j+1} - w_j) - (P^z)^{-1} v_j, \\ y_{j+1} &= P^y (P^z)^{-1} r^z + S w_{j+1} + T w_j - (P^z)^{-1} P^y v_j. \end{aligned}$$

*Proof.* From Fig. 6 follows  $u_j = S C \eta_j + S C r^z - S C w_j$  and  $e_j^z = (I - P^z S C) r^z - S P^z C \eta_j + P^z S C w_j - v_j$ . Substitution of  $e_j^z$  in (3) yields  $\eta_{j+1}$ . The result follows by substitution of  $\eta_{j+1}$  in  $u_{j+1}$  and  $y_{j+1}$ .  $\square$

**Corollary 5.** If the disturbances are trial-invariant, i.e.,  $w_{j+1} = w_j = w$  and  $v_{j+1} = v_j = v$ , then the tracking error  $e_{j+1}^z = 0$ , yielding perfect tracking performance. The output  $y_{j+1} = P^y (P^z)^{-1} r^z + w - (P^z)^{-1} P^y v$ .

**Corollary 6.** If the disturbances are zero, the feedforward  $\eta_{j+1} = (L - I)r^z$ . The latter is depended on the feedback controller since  $L = [P^z S C]^{-1}$ . This is in contrast to the 2-DOF inferential ILC solution, see the performance analysis in Section III-C, where  $f_{j+1} = (P^z)^{-1} r^z$ .

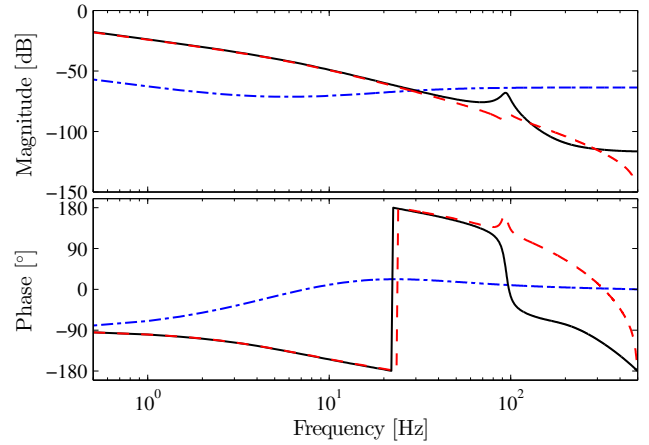


Fig. 8. Models  $P^z$  (solid black),  $P^y$  (dashed red), and 1-DOF feedback controller  $C \cdot 10^{-6}$  (dashed-dotted blue).

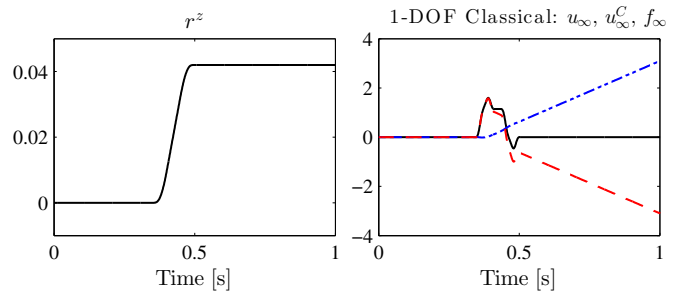


Fig. 9. Left: reference  $r^z$  (solid black). Right: converged command signals  $u_\infty$  (solid black),  $f_\infty$  (dashed red), and  $u_\infty^C$  (dashed-dotted blue) for the classical non-inferential 1-DOF structure, revealing the conflicting control objectives.

## V. SIMULATION EXAMPLE

First, the conflicting control objectives between  $C$  and the ILC in the structure of Fig. 2 are illustrated with a simulation example. Then, the 2-DOF inferential ILC structure Fig. 6 is compared with the 1-DOF structure in Fig. 7.

A model of the Medium Positioning Drive (MPD) in Fig. 1 has been identified on a commercial wide-format printer. A 1-DOF feedback controller  $C$  as in Fig. 2 is given. The respective Bode diagrams of  $P^z$ ,  $P^y$  and  $C$  are shown in Fig. 8. The Bode diagram shows that the dynamics of  $P^z$  and  $P^y$  are almost identical for frequencies below 20 Hz. For frequencies higher than 20 Hz the dynamics are clearly different. The 1-DOF feedback controller is a standard PID controller with a first order low-pass filter.

1) *Classical structure:* The task of the MPD is to shift the paper with a fixed step size. The reference is shown in Fig. 9 (left). A simulation using the classical 1-DOF non-inferential control structure in Fig. 2 is invoked using inverse-model ILC, the converged command signals are presented in Fig. 9 (right). It clearly shows that the feedback command signal  $u_\infty^C$  is growing unbounded, with opposite sign of the ILC command signal  $f_\infty$ . The input to the system  $u_\infty = u_\infty^C + f_\infty = (P^z)^{-1}$ .

2) *Inferential control structures:* The type of 2-DOF controller used is the configuration in Fig. 3, known as indirect

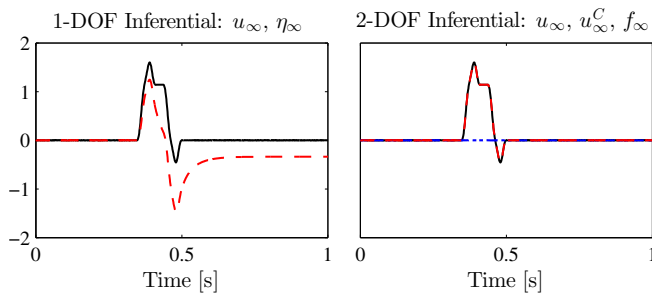


Fig. 10. Left: converged command signals  $u_\infty$  (solid black) and  $\eta_\infty \cdot 300$  (dashed red) for the inferential 1-DOF structure. Right: converged command signals  $u_\infty$  (solid black),  $f_\infty$  (dashed red), and  $u_\infty^C$  (dashed-dotted blue) for the inferential 2-DOF structure.

control and involves a transformation of the reference. The 2-DOF controller  $[C_1, C_2]$  in Fig. 6 is given by  $C_2 = C$  and  $C_1 = P^y(P^z)^{-1}C$ , with  $C$  the 1-DOF feedback controller in Fig. 8. The learning updates are given in (1) and (3) for the 2-DOF and 1-DOF structures, respectively. The disturbances  $w_j = v_j = 0$ .

The simulation results are presented in Fig. 10. The converged command signals for the two structures are shown: 1-DOF inferential (left) and the 2-DOF inferential structure (right). The achieved errors  $e_\infty^z = 0$  for all approaches, and are hence not shown. First, notice that  $u_\infty = (P^z)^{-1}r$  for both structures, as expected from Theorems 2 and 4. Also notice that the conflict that appeared in the classical structure, see Fig. 9 (right), is resolved.

The main advantage of the 2-DOF structure is that the command signal of the ILC has the role of ordinary feedforward and can be used for instance for calibration purposes. This can be seen in Fig. 10 (right), the feedback controller is inactive during the execution of the reference. A disadvantage may be that the conflicting objectives between the ILC and  $C$  persists in case of trial-invariant output-disturbances  $v_j$  and  $w_j$ , as elaborated on in Remark 1. If the output disturbances are significant and trial-invariant in practice, then a solution is to use the 1-DOF structure, at the expense of a controller-dependent ILC command signal  $\eta_\infty$ , see Fig. 10 (left).

## VI. CONCLUSION

In this paper, the aspects of ILC for inferential control are analyzed. Two frameworks are proposed. For the first framework, recent developments in the robust inferential control of mechatronic systems are exploited, and resorts to a 2-DOF inferential feedback structure with ILC. This solution requires redesign of the feedback controller which in practice may not always be possible. The second solution is in the common 1-DOF control structure where the ILC is specifically designed to address the inferential control problem.

The results include a mathematical analysis of the performance with the system subject to disturbances. A simulation example using a model of a medium positioning drive of a wide-format printer supports the results.

Ongoing research focuses on: the actual implementation of the inferential norm-optimal ILC in an experimental system,

analysis of the robustness against model uncertainty, and an in-depth stability analysis of the inferential control configurations with conflicting control objectives.

## ACKNOWLEDGMENT

The authors would like to acknowledge the fruitful discussions with late Okko Bosgra and Sjirk Koekebakker that have significantly contributed to the results.

This work is supported by Océ Technologies, P.O. Box 101, 5900 MA Venlo, The Netherlands. This work is also supported by the Innovational Research Incentives Scheme under the VENI grant ‘‘Precision Motion: Beyond the Nanometer’’ (no. 13073) awarded by NWO (The Netherlands Organisation for Scientific Research) and STW (Dutch Science Foundation).

## REFERENCES

- [1] J. R. Parrish and C. B. Brosilow, ‘‘Inferential Control Applications,’’ *Automatica*, vol. 21, no. 5, pp. 527–538, 1985.
- [2] T. Oomen, O. Bosgra, and M. van de Wal, ‘‘Identification for Robust Inferential Control,’’ In *Proc. Joint Conference on Decision and Control and Chinese Control Conference, Shanghai, China*, pp. 2581–2586, 2009.
- [3] T. Oomen, J. van de Wijdeven, and O. Bosgra, ‘‘System Identification and Low-Order Optimal Control of Intersample Behavior in ILC,’’ *IEEE Trans. Automat. Contr.*, pp. 2734–2739, 2011.
- [4] J. Bolder, B. Lemmen, S. Koekebakker, T. Oomen, O. Bosgra, and M. Steinbuch, ‘‘Iterative Learning Control with Basis Functions for Media Positioning in Scanning Inkjet Printers,’’ *Proc. Multi-conf. Syst. Contr., Dubrovnik, Croatia*, pp. 1255–1260, 2012.
- [5] D. Bristow, M. Tharayil, and A. Alleyne, ‘‘A Survey of Iterative Learning Control: a Learning-based Method for High-performance Tracking Control,’’ *IEEE Contr. Syst. Mag.*, vol. 26, pp. 96–114, 2006.
- [6] D. Gorinevsky, ‘‘Loop Shaping for Iterative Control of Batch Processes,’’ *IEEE Contr. Syst. Mag.*, vol. 22, pp. 55–65, 2002.
- [7] Y. Chen, K. L. Moore, J. Yu, and T. Zhang, ‘‘Iterative Learning Control and Repetitive Control in Hard Disk Drive Industry - A Tutorial,’’ *Int. J. Adapt. Contr. Sign. Proc.*, vol. 23, pp. 325–343, 2008.
- [8] K. L. Moore, *Iterative Learning Control for Deterministic Systems*. Springer-Verlag, 1993.
- [9] S. Gunnarsson, M. Norrlöf, E. Rahic, and M. Özbek, ‘‘On the use of Accelerometers in Iterative Learning Control of a Flexible Robot Arm,’’ *Int. J. Contr.*, vol. 80, pp. 363–373, 2007.
- [10] J. Wallén, M. Norrlöf, and S. Gunnarsson, ‘‘A Framework for Analysis of Observer-based ILC,’’ *Asian Journal of Control*, vol. 13, pp. 3–14, 2011.
- [11] T. Oomen, ‘‘System Identification for Robust and Inferential Control with Applications to ILC and Precision Motion Systems,’’ *Ph.D. Thesis, Eindhoven University of Technology*, 2010.
- [12] D. Roover, O. Bosgra, and M. Steinbuch, ‘‘Internal-model-based Design of Repetitive and Iterative Learning Controllers for Linear Multivariable Systems,’’ *Int. J. Contr.*, vol. 73, pp. 914–929, 2000.
- [13] S. Skogestad and I. Postlethwaite, *Multivariable Feedback Control: Analysis and Design*. Wiley, 2005.
- [14] S. Devasia, ‘‘Should Model-Based Inverse Inputs Be Used as Feedforward Under Plant Unvertainty?’’ *IEEE Trans. Automat. Contr.*, vol. 47, pp. 1865–1871, 2002.
- [15] B. Barmish and A. Galimidi, ‘‘Robustness of Luenberger Observers: Linear Systems Stabilized via Non-linear Control,’’ *Automatica*, vol. 22, pp. 413–423, 1986.
- [16] N. Amann, D. Owens, and E. Rogers, ‘‘Iterative Learning Control Using Optimal Feedback and Feedforward Actions,’’ *Int. J. Contr.*, vol. 65, pp. 277–293, 1996.
- [17] S. Gunnarsson and M. Norrlöf, ‘‘On the design of ILC algorithms using optimization,’’ *Automatica*, vol. 37, pp. 2011–2016, 2001.
- [18] K. Barton, D. Hoelzle, A. Alleyne, and A. Johnson, ‘‘Cross-Coupled Iterative Learning Control of Systems with Dissimilar Dynamics: Design and Implementation for Manufacturing Applications,’’ *Int. J. Contr.*, vol. 84, pp. 1223–1233, 2011.
- [19] P. Janssens, G. Pipeleers, and J. Swevers, ‘‘A Data-Driven Constrained Norm-Optimal Iterative Learning Control Framework for LTI Systems,’’ *IEEE Trans. Contr. Syst. Techn.*, vol. 21, pp. 546–551, 2013.